QCD description of diffractive ρ meson electroproduction

A. D. Martin, M. G. Ryskin,* and T. Teubner
Department of Physics, University of Durham, Durham, DH1 3LE, United Kingdom

(Received 24 September 1996)

We critically review the QCD predictions for the cross sections σ_L and σ_T for diffractive ρ meson electroproduction in longitudinally and transversely polarized states in the DESY HERA energy region. We show that both perturbative and nonperturbative approaches, which involve convolution with the ρ meson wave function, predict values of σ_T which fall off too quickly with increasing Q^2, in comparison with the data. We present a perturbative QCD model based on the open production of light $q\bar{q}$ pairs and parton-hadron duality, which describes all features of the data for ρ electroproduction at high Q^2 and, in particular, predicts a satisfactory Q^2 behavior of σ_L/σ_T. We find that precise measurements of the latter can give valuable information on the Q^2 behavior of the gluon distribution at small x. [S0556-2821(97)00807-2]

PACS number(s): 13.60.Le, 12.38.Bx

I. INTRODUCTION

The results of the measurements of ρ meson electroproduction, $\gamma^* p \rightarrow \rho p$, are intriguing. These are coming from the H1 [1] and ZEUS [2,3] experiments at the DESY electron-proton collider HERA, and should be considered in conjunction with the earlier measurements of New Muon Collaboration (NMC) [4] at lower energies. We may briefly summarize the main features of the observed behavior of the cross section $\sigma(\gamma^* p \rightarrow \rho p)$ as follows:

(i) $\sigma \sim 1/Q^5$ for $7 < Q^2 < 30$ GeV^2.

(ii) $\sigma \sim W^{0.8}$ for[1] $12 < W < 140$ GeV.

(iii) $\sigma_L/\sigma_T \sim 2-4$ weakly rising with Q^2 for $6 < Q^2 < 20$ GeV^2.

(iv) $d\sigma/dt \sim e^{bt}$ with $b \simeq 5-6$ GeV^{-2} for $Q^2 > 10$ GeV^2, as compared to $b \simeq 9$ GeV^{-2} for $Q^2 = 0$.

As usual, Q^2 is the virtuality of the photon, W is the center-of-mass energy of the $\gamma^* p$ system, and t is the square of the four-momentum transfer. The ρ meson is observed through its 2π decay. If there are sufficient events, then the angular distribution of the decay products allows the measurement of the components σ_L and σ_T of the cross section, which describe ρ production in longitudinally and transversely polarized states, respectively. As we shall see, the measurement of the Q^2 dependence of σ_L/σ_T is particularly informative. The present data (iii) have large errors, but already indicate the general trend.

Observations (ii) and (iv) imply the validity of perturbative QCD for the description of high energy ρ electroproduction. Observation (iv) means that the size of the system (the $\gamma^* \rightarrow \rho$ Pomeron vertex) decreases with Q^2, and that at large Q^2 we do indeed have a short-distance interaction so that perturbative QCD is justified. In fact, the measurement of the slope $b \simeq 5-6$ GeV^{-2} is approximately equal to that expected from the size of the proton, which is consistent with the hypothesis that at large Q^2 the size of the $\gamma^* \rightarrow \rho$ vertex is close to zero. From observation (ii) we see that the exponent of the $\sigma \sim W^n$ behavior has changed from the ''soft'' pomeron value[2] $n = 4[\alpha_P(t) - 1] \simeq 0.2$ observed in ρ photoproduction ($Q^2 = 0$), to a value $n = 4\lambda \simeq 0.8$ at high Q^2 which is consistent with the gluon density, $xg \sim x^{-\lambda}$, extracted[3] from the observed QCD scaling violations of F_2. Moreover, it is in line with the $\sigma \sim W^{0.8}$ behavior observed in J/ψ photoproduction, where perturbative QCD is expected to be applicable due to the sizable charm quark mass.

Here, we explore the implications of all the observed properties (i)–(iv) for the QCD description of ρ electroproduction at HERA. Before we present our detailed study, it is useful to give a brief overview of the situation. We begin with the Q^2 dependence of $\sigma(\gamma^* p \rightarrow \rho p)$. We will show that for ρ meson electroproduction at high Q^2, perturbative QCD should be applicable to σ_T as well as to σ_L. The leading order perturbative QCD prediction for electroproduction in longitudinally polarized states is [8,9]

$$\sigma_L \sim \frac{[xg(x,Q^2)]^2}{Q^6} \sim \frac{(Q^2)^{2\gamma}}{Q^6} \sim \frac{1}{Q^{4.8}} \tag{1}$$

for $Q^2 \gg m_\rho^2$, where $x = Q^2/W^2$ and γ is the anomalous dimension of the gluon density, $xg(x,Q^2) \sim (Q^2)^\gamma$. For the relevant range of x, $10^{-3} \lesssim x \lesssim 10^{-2}$, we have taken,[4] for the purposes of illustration, the representative average value $\gamma = 0.3$. So, the QCD prediction for σ_L is consistent with the Q^2 behavior of the data. This is not the case for σ_T. The

*Permanent address: Laboratory of Theoretical Nuclear Physics, St. Petersburg Nuclear Physics Institute, Gatchina, St. Petersburg 188350, Russia.

[1]This behavior is observed from the NMC experiment at $W \simeq 13$ GeV right through the HERA energy range, 40–140 GeV.

[2]Corresponding to $\alpha_P(0) \simeq 1.08$.

[3]The Martin-Roberts-Stirling (MRS) parton sets, which best describe the recent HERA measurements of F_2 [5] and other data, are MRS(A$'$) [6] and MRS(R2) [7]. For these the effective value of λ increases from about 0.2 to 0.3 as Q^2 increases from 10 to 50 GeV^2.

[4]From the most recent sets of partons [6,7] we find $\gamma \simeq 0.25$ rising to $\gamma \simeq 0.4$ as x decreases from 10^{-2} to 10^{-3} for $Q^2 \approx 10$ GeV^2. Of course, in the numerical analysis of Sec. VI the true x and Q^2 dependence of γ is automatically included.

prediction for σ_T appears to be too small and to fall too rapidly with increasing Q^2. If only the leading-twist component of the light-cone wave function[5] of the ρ is taken into account, then

$$\sigma_T \sim \frac{m^2}{Q^2}\sigma_L \sim \frac{1}{Q^{6.8}}, \tag{2}$$

where m is the current (light) quark mass. Although the leading twist is specified by the QCD sum rules, the next twist is not known. However, we can make reasonable assumptions to estimate its effect. We find that its inclusion has the effect of replacing m^2 in Eq. (2) by a factor of the order of m_ρ^2. Even considering the uncertainties, the value predicted for σ_L/σ_T is still much too big and has the wrong Q^2 dependence in comparison with the data. We elaborate the above arguments in Sec. II.

It is frequently claimed that perturbative QCD is not applicable for σ_T and that its behavior is of nonperturbative origin, see, for example, Ref. [9]. But in this case we would expect the same slope b as that in photoproduction and a ''soft'' $W^{0.2}$ behavior. Moreover, nonperturbative QCD predicts a $1/Q^8$ or stronger falloff of σ_T with increasing Q^2. Recall that these features are not observed in the data. A further discussion of the nonperturbative approach is given in Sec. III.

Here, we present a resolution of the problem, which is based on the application of the hadron-parton duality hypothesis to the production of open $q\bar{q}$ pairs.[6] First, we recall the hadron-parton duality hypothesis for the process $e^+e^- \to$ hadrons. In this case the hypothesis gives

$$\left\langle \sum_h \sigma(e^+e^- \to \gamma^* \to h) \right\rangle_{\Delta M^2} \simeq \left\langle \sum_q \sigma(e^+e^- \to \gamma^* \to q\bar{q}) \right\rangle_{\Delta M^2}, \tag{3}$$

that is, the total hadron production ($h=\rho,\omega,\ldots$), averaged over a mass interval ΔM^2 (typically $\sim 1\ \mathrm{GeV}^2$), is well represented by the partonic cross section. This duality has been checked [11] down to the lowest values of $\sqrt{s}$. We may, therefore, expect the duality to apply to diffractive ρ electroproduction for $q\bar{q}$ produced in the invariant mass interval containing the ρ meson, $M^2 \lesssim 1$–$1.5\ \mathrm{GeV}^2$. In this domain the more complicated partonic states ($q\bar{q}+g, q\bar{q}+2g, q\bar{q}+q\bar{q},\ldots$) are heavily suppressed, while on the hadronic side the 2π (and to a lesser extent the 3π) states are known to dominate. Thus, for low M^2 we mainly have

$$\gamma^* \to q\bar{q} \to 2\pi \tag{4}$$

or, in other words,

$$\sigma(\gamma^* p \to \rho p) \simeq 0.9 \sum_{q=u,d} \int_{M_a^2}^{M_b^2} \frac{d\sigma[\gamma^* p \to (q\bar{q})p]}{dM^2} dM^2, \tag{5}$$

[5]The twist of the ρ wave function should not be confused with that of the operator which corresponds to the γp amplitude.

[6]The use of duality to predict longitudinal ρ production was mentioned in Ref. [10].

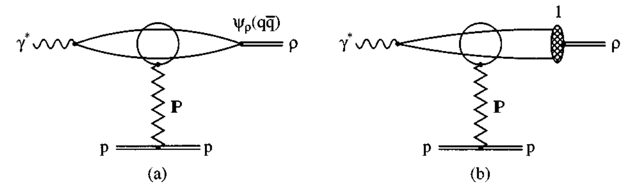

FIG. 1. Alternative mechanisms for ρ meson electroproduction: (a) involves a convolution of the $\psi_\gamma(q\bar{q})$ and $\psi_\rho(q\bar{q})$ wave functions, whereas (b) is based on open $q\bar{q}$ production and parton-hadron duality. At high Q^2 the ''Pomeron'' exchange in this picture really stands for the exchange of two gluons in the t channel.

where the limits M_a^2 and M_b^2 are chosen so that they appropriately embrace the ρ meson mass region with $M_b^2 - M_a^2 \sim 1\ \mathrm{GeV}^2$. The factor 0.9 is included to allow for ω production. This duality model is predictive. In Sec. IV we present the QCD formula for open $q\bar{q}$ electroproduction via two-gluon exchange, and in Sec. V we discuss their general structure. In particular, we show how the scale dependence of the gluon density softens the $\sigma_L/\sigma_T \sim Q^2$ growth with increasing Q^2. The numerical predictions are presented in Sec. VI. There we calculate diffractive $u\bar{u}$ and $d\bar{d}$ electroproduction and use the duality hypothesis to make detailed predictions of the Q^2 dependence of both σ_L and σ_T for ρ meson electroproduction at HERA; results whose general structure was anticipated in the discussion of Sec. V.

In short, we argue that the convolution of the $q\bar{q}$ wave function (produced by the γ^*), with any reasonable ρ meson wave function, would yield a prediction for σ_T which is in disagreement with the data. Rather, we claim that ρ electroproduction proceeds via *open* $u\bar{u}$, $d\bar{d}$ production at low M^2, which has a different structure. Some long time after the interaction with the proton, confinement distorts the $q\bar{q}$ state and forces it to be the ρ meson, as there are no other possibilities. That is, the suppression due to the small wave function overlap $\langle q\bar{q}|\rho^0\rangle$ is not operative. We depict the situation in Fig. 1.

II. STANDARD PERTURBATIVE APPROACH TO THE Q^2 BEHAVIOR OF $\sigma_{T,L}(\rho)$

First, we wish to sketch the derivation of the perturbative QCD prediction for σ_T shown in Eq. (2),

$$\sigma_T(\gamma^* p \to \rho p) \sim [xg(x,Q^2)]^2/Q^8 \tag{6}$$

for $Q^2 \gg m_\rho^2$, and to show that it is infrared stable. We must, therefore, study the $\gamma^* \to \rho$ Pomeron vertex (or so-called impact factor) of Fig. 1(a), which we denote by J_T. We shall also consider J_L. The factors are given by the convolution of the wave functions $\psi_\gamma(q\bar{q})$ and $\psi_\rho(q\bar{q})$. It is found that [9,12]

$$J_i = f_\rho \int \frac{dz\, dk_T^2}{\varepsilon^2 + k_T^2} \psi_\rho^i(z,k_T^2) B_i, \tag{7}$$

with $i=T$ or L. The quantity f_ρ is the ρ meson decay constant and the term ε^2 in the quark propagator is

$$\varepsilon^2 = z(1-z)Q^2 + m^2, \tag{8}$$

where m is the current quark mass. B_i are the helicity factors[7] coming from the quark loop, see Fig. 1(a),

$$B_L = 2z(1-z)\sqrt{Q^2}, \tag{9}$$

$$B_T = -m. \tag{10}$$

$\psi_\rho(z,k_T^2)$ is the momentum representation of the ρ meson wave function; z and $\mathbf{k}_T$ are the Sudakov and transverse momentum components carried by one of the quarks with respect to the photon. The other quark has components $1-z$ and $-\mathbf{k}_T$.

The wave functions $\psi_\rho^{L,T}$ decrease slowly with k_T^2 and the convergence of the integral in Eq. (7) is provided only by the denominator $\varepsilon^2 + k_T^2$. We, therefore, introduce an integrated wave function

$$\phi_\rho^i(z) \equiv \int^{\varepsilon^2} dk_T^2 \psi_\rho^i(z,k_T^2), \tag{11}$$

defined by the scale $\mu^2 = \varepsilon^2$ at which the integral ceases to converge. The quantities ϕ_ρ^i are called the leading-twist, light-cone ρ meson wave functions and have been well studied in the framework of QCD sum rules [13,14]. As $Q^2 \to \infty$ (that is $\varepsilon^2 \to \infty$), we have

$$\phi_\rho^i(z) \to 6z(1-z) \tag{12}$$

for both $i = T,L$. Their behavior at finite scales can be found in Refs. [13,14], but in any case the ϕ_ρ vanish at least as fast as z as $z \to 0$ and as $1-z$ as $z \to 1$. We may rewrite the impact factors (7) in terms of the integrated wave functions $\phi_\rho^i(z)$. We obtain

$$J_i \approx f_\rho \int \frac{dz}{\varepsilon^2} \phi_\rho^i(z) B_i. \tag{13}$$

Finally, we must convolute J_i with the $q\bar{q}$-proton interaction amplitude T given by the "hard" QCD Pomeron (or two-gluon exchange ladder). The amplitude T behaves as

$$\frac{1}{s}\mathrm{Im}T = \sigma_{q\bar{q}-p} \sim \frac{xg(x,\varepsilon^2)}{\varepsilon^2} \sim (\varepsilon^2)^{\gamma-1}, \tag{14}$$

where recall that the scale is $\varepsilon^2 = z(1-z)Q^2 + m^2$, and where $\gamma(x)$ is the anomalous dimension of the gluon. Thus, the amplitudes for ρ electroproduction from transversely $(i=T)$ and longitudinally $(i=L)$ polarized photons are

$$A_i = J_i \otimes T = f_\rho \int \frac{dz}{(\varepsilon^2)^{2-\gamma}} \phi_\rho^i(z) B_i, \tag{15}$$

which yield the following Q^2 behavior of the cross sections

$$\sigma_T \sim |A_T|^2 \sim [m/(Q^2)^{2-\gamma}]^2 \sim m^2/Q^{6.8}, \tag{16}$$

$$\sigma_L \sim |A_L|^2 \sim Q^2[1/(Q^2)^{2-\gamma}]^2 \sim 1/Q^{4.8}. \tag{17}$$

For illustration, we have again set the gluon anomalous dimension $\gamma = 0.3$. We emphasize that the integral in Eq. (15) is convergent for A_T (for any $\gamma > 0$), as well as for A_L. Thus, $\varepsilon^2 \sim Q^2$ and perturbative QCD is valid not only for σ_L [where we have additional convergence due to $B_L \sim z(1-z)$], but *also* for σ_T.

We note that while the prediction for the relative Q^2 dependence of σ_T and σ_L is meaningful (although not supported by the data), the value for the ratio

$$\frac{\sigma_T}{\sigma_L} \sim \frac{m^2}{Q^2} \tag{18}$$

(which is in gross disagreement with the data) is not a reliable estimate. The reason is that the current u,d quark masses are very small ($m \lesssim 7$ MeV) and that, therefore, we must consider how the non-leading-twist contribution to $\psi_\rho^T(z,k_T^2)$ will modify the prediction for σ_T. The nonleading twist is not known. However, it is reasonable to assume that instead of two variables, the ρ wave function ψ_ρ^T depends on only one variable, namely, the invariant mass of the $q\bar{q}$ pair[8]

$$M^2 = \frac{k_T^2}{z(1-z)}, \tag{19}$$

where we neglect m^2. Then, after some algebra, it is possible to show that the impact factor J_T can be written in the form of Eq. (15) with $\phi_\rho^T = 6z(1-z)$, and that the helicity factor becomes

$$B_T = -\tfrac{1}{2} m_\rho [z^2 + (1-z)^2], \tag{20}$$

rather than the very small "leading-twist" prediction given in Eq. (10). The reason that we still obtain a definite prediction for J_T, again in terms of f_ρ, is due to the fact that this same non-leading-twist component of ψ_ρ^T describes the decay $\rho_T \to e^+e^-$, that is, the k_T integral over the quark loop describing the ρ_T decay is the same integral that occurs in the impact factor J_T for $Q^2 \gg m_\rho^2$. In this way we are able to normalize the nonleading twist to the observed width of the decay, that is, to the decay constant f_ρ.

If we estimate the ρ electroproduction amplitude A_T of Eq. (15), using the modified form (20) of B_T, then we obtain

$$\frac{\sigma^T}{\sigma_L} = c\,\frac{m_\rho^2}{Q^2}, \tag{21}$$

with $c \sim 2$. The precise value of c depends on the actual forms of $\phi_\rho^{T,L}(z)$ at the experimentally relevant scales, $\mu^2 \sim 10$ GeV^2, which are far from the asymptotic region where $\phi_\rho^{T,L}(z) = 6z(1-z)$. In our approximate estimate of $c \sim 2$ we have used the $\phi_\rho^{T,L}(z)$ wave functions of Ref. [14]. Although a considerable improvement on Eq. (18), the prediction (21) for the ratio σ^T/σ^L is still much smaller than the observed ratio and, as before, decreases more rapidly with

[7]The vertex satisfies s channel (quark) helicity conservation. In general, for $t \neq 0$ we would also have off-diagonal helicity factors, $B(\gamma_T,\rho_L)$ and $B(\gamma_L,\rho_T)$.

[8]This hypothesis is very natural from a dispersion relation viewpoint [15].

Q^2 than that indicated by the data [1,2,4]. In short, the standard perturbative QCD predictions for $\sigma_T(\gamma^* p \to \rho p)$ are not in agreement with the observations.

III. NONPERTURBATIVE APPROACH TO THE Q^2 DEPENDENCE OF $\sigma_T(\rho)$

It has been argued that the main contribution to σ_T comes from the nonperturbative region [9]. Let us disregard the fact that the perturbative integral (15) is convergent for σ_T and suppose that nonperturbative effects dominate. In order to obtain nonperturbative contributions associated with small ($\sim \mu^2$) virtualities, we must get contributions from the endpoint regions of integration

$$z \lesssim \mu^2/Q^2 \quad \text{and} \quad 1-z \lesssim \mu^2/Q^2. \tag{22}$$

Only then will we sample small scales $\varepsilon^2 \sim \mu^2$ and large distances $\rho \sim 1/\varepsilon \sim 1/\mu$. However, for large distances the quark effectively has a constituent mass $m_q \sim \frac{1}{2} m_\rho$ and the nonrelativistic wave function, $\phi_\rho^T(z) \sim \delta(z-\frac{1}{2})$, is appropriate. Certainly, $\phi_\rho^T(z)$ decreases exponentially or, at least as a large power, as $z \to 0$ or $z \to 1$. Thus, the contribution from the regions (22) should be strongly suppressed. Even if $\phi_\rho^T(z) \sim z(1-z)$, as in Eq. (12), we would obtain, from Eq. (13) with $\varepsilon \sim \mu$,

$$\sigma_T(\text{nonpert}) \sim \left[\frac{1}{\mu^2} \int_0^{\mu^2/Q^2} dz\, \phi_\rho^T(z) B_T \right]^2 \sim \frac{1}{Q^8}. \tag{23}$$

Thus, for the actual nonperturbative prediction we would expect an even faster falloff with increasing Q^2.

IV. QCD MODEL FOR $\sigma_{L,T}(\rho)$ VIA OPEN $q\bar{q}$ PRODUCTION

The above discussion suggests that the problem in successfully describing ρ meson electroproduction may be associated with having to convolute with a ρ meson wave function, which inevitably leads to a form-factor-like suppression of the form $|\langle q\bar{q}|\rho^0\rangle|^2 \sim 1/Q^4$. Here, we study an alternative and physically compelling mechanism for ρ electroproduction based on the production of $u\bar{u}$ and $d\bar{d}$ pairs in a broad mass interval containing the ρ meson. In this mass interval, phase space forces these $q\bar{q}$ pairs to hadronize dominantly into 2π states, with only a small amount of 3π production. Moreover, provided the $q\bar{q}$-proton interaction does not distort the spin, we expect that the process $\gamma^* \to q\bar{q} \to 2\pi$ will dominantly produce 2π systems with $J^P = 1^-$. The calculation of the diffractive electroproduction of $q\bar{q}$ pairs, therefore, allows, via the parton-hadron duality hypothesis, a detailed prediction of the structure of ρ meson electroproduction.

The formula for the diffractive production of open $q\bar{q}$ pairs is given in Refs. [16,17]. For light quarks we may safely put the current quark mass $m=0$. The process is shown in Fig. 2. We use the same notation as in Ref. [16], so the scale at which the gluon distribution is sampled is denoted

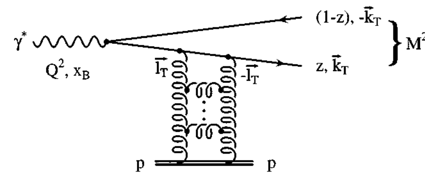

FIG. 2. Diffractive open $q\bar{q}$ production in high energy $\gamma^* p$ collisions, where z is the fraction of the energy of the photon that is carried by the quark. The transverse momenta of the outgoing quarks are $\pm \vec{k}_T$, and those of the exchanged gluons are $\pm \vec{\ell}_T$.

$$K^2 = z(1-z)Q^2 + k_T^2 = \frac{k_T^2}{1-\beta}, \tag{24}$$

where the last equality follows since $z(1-z) = k_T^2/M^2$ and

$$\beta \equiv \frac{Q^2}{Q^2+M^2}. \tag{25}$$

Note that the scale K^2 plays the role that ε^2 played for exclusive vector meson production [cf. Eq. (8)], and that it determines the transverse distances $b_T \sim 1/K$ that are typically sampled in the process. It is convenient to replace the dk_T^2 integration over the quark transverse momenta k_T in formulas (40) and (41) in Ref. [16] by an integration over dK^2. Then, it is straightforward to show that these formulas giving the $\gamma^*_{L,T} p \to (q\bar{q}) p$ cross sections in the forward direction ($t=0$) may be written in the form

$$\frac{d^2\sigma_L}{dM^2 dt} = \frac{4\pi^2 e_q^2 \alpha}{3} \frac{Q^2}{(Q^2+M^2)^4} \times \int_{K_0^2}^{(1/4)(Q^2+M^2)} \frac{dK^2 K^2}{\sqrt{1-4K^2/(Q^2+M^2)}} [I_L(K^2)]^2, \tag{26}$$

$$\frac{d^2\sigma_T}{dM^2 dt} = \frac{4\pi^2 e_q^2 \alpha}{3} \frac{M^2}{(Q^2+M^2)^3} \times \int_{K_0^2}^{(1/4)(Q^2+M^2)} \frac{dK^2 (1-2\beta K^2/Q^2)}{\sqrt{1-4K^2/(Q^2+M^2)}} [I_T(K^2)]^2, \tag{27}$$

where α is the electromagnetic coupling. The quantities $I_{L,T}$ are the integrations over the transverse momenta $\pm \ell_T$ of the exchanged gluons (see Fig. 2)

$$I_L(K^2) = K^2 \int \frac{d\ell_T^2}{\ell_T^4} \alpha_S(\ell_T^2) f(x, \ell_T^2) \left(\frac{1}{K^2} - \frac{1}{K_\ell^2} \right), \tag{28}$$

$$I_T(K^2) = \frac{K^2}{2} \int \frac{d\ell_T^2}{\ell_T^4} \alpha_S(\ell_T^2) f(x, \ell_T^2) \times \left(\frac{1}{K^2} - \frac{1}{2k_T^2} + \frac{K^2 - 2k_T^2 + \ell_T^2}{2k_T^2 K_\ell^2} \right), \tag{29}$$

where $x = (Q^2+M^2)/W^2$,

$$K_{\ell}^2 \equiv \sqrt{(K^2+\ell_T^2)^2-4k_T^2\ell_T^2}, \tag{30}$$

and $f(x,\ell_T^2)$ is the unintegrated gluon distribution of the proton. We will use formulas (26) and (27) to predict ρ meson electroproduction. They involve integration over the quark k_T^2 (or K^2) and over the ℓ_T^2 of the exchanged gluons. As we are dealing with a diffractive process we see that the cross sections have a quadratic sensitivity to the gluon density.

It is useful to inspect the leading $\ln K^2$ approximation to the $d\ell_T^2$ integrations of Eqs. (28) and (29). In this approximation it is assumed that the main contributions to the integrals come from the domain $\ell_T^2 \lesssim K^2$, and so, on expanding the integrands, we obtain[9]

$$I_L^{LLA}=I_T^{LLA}=\frac{\alpha_S(K^2)}{K^2}\int^{K^2}\frac{d\ell_T^2}{\ell_T^2}f(x,\ell_T^2)=\frac{\alpha_S(K^2)}{K^2}xg(x,K^2). \tag{31}$$

By analogy with Eq. (14), we see that $I_{L,T}$ are essentially the cross sections for the $(q\bar{q})_{L,T}$ interaction with the proton. Of course, in the calculations presented in Sec. VI we do not use the leading log approximation, but instead we perform the explicit $d\ell_T^2$ integrations over $f(x,\ell_T^2)=\partial[xg(x,\ell_T^2)]/\partial\ln\ell_T^2$ given in Eqs. (28) and (29). We treat the infrared region using the linear approximation described in Ref. [16] for low ℓ_T^2 values (that is, $\ell_T^2<\ell_0^2$). We find stability of the results to reasonable variations of the choice of ℓ_0^2.

V. INSIGHT INTO THE STRUCTURE OF THE CROSS SECTIONS $\sigma_{L,T}$

In Sec. VI we show the predictions for the Q^2 behavior of σ_L and σ_T for ρ electroproduction, which are obtained from the numerical evaluation of Eqs. (26) and (27) integrated over the ρ mass region. However, it is informative to anticipate some of the general features of the results. First, we study the infrared convergence of the dK^2 integrations of Eqs. (26) and (27). We note from the approximate forms of $I_{L,T}$ in Eq. (31) that

$$I_i \sim x^{-\lambda}(K^2)^{\gamma}/K^2, \tag{32}$$

where λ and γ are the effective exponents of the gluon defined by

$$xg(x,K^2)\sim x^{-\lambda}(K^2)^{\gamma}. \tag{33}$$

We see that the integration (26) is infrared convergent provided that $\gamma>0$ as $K^2\to 0$, whereas we require $\gamma>0.5$ to ensure the convergence of Eq. (27). How does the value of γ depend on K^2? At high energy W (that is, $x\approx Q^2/W^2\to 0$), the gluon $g(x,K^2)$ increases much faster as x decreases for large K^2 ($xg\sim x^{-\lambda}$ with $\lambda \gtrsim 0.3$) than it does for small K^2. Thus, the effective anomalous dimension γ increases when x and K^2 decrease. The behavior is evident in Fig. 3 which shows the values of γ (as a function of x for selected K^2), obtained from two recent sets of partons. For

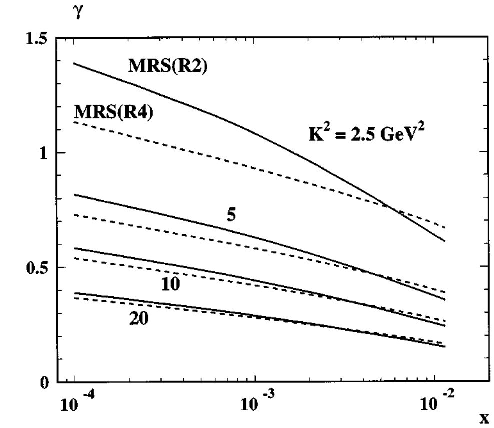

FIG. 3. The continuous curves show the effective anomalous dimension γ of the gluon [defined by $xg(x,K^2)\sim(K^2)^{\gamma}$], determined from the MRS(R2) set of partons [7] for $K^2=2.5$, 5, 10, and 20 GeV^2. The dashed curves correspond to the values of γ for the R4 set of partons.

example, let us take a typical value $x\approx Q^2/W^2=10^{-3}$ relevant for the measurements at HERA (say $Q^2=10$ GeV^2 and $W=100$ GeV). We see from Fig. 3 that γ increases from 0.3, 0.45, 0.6 to 1 as K^2 decreases from about 20, 10, 5 to 2.5 GeV^2. The infrared convergence requirement, $\gamma>0.5$, of Eq. (27) is, therefore, already satisfied when K^2 has decreased to 8 GeV^2. In general, the behavior of γ with K^2 amply provides, via Eq. (32), the infrared convergence of Eq. (27), as well as that of Eq. (26). This explains the reason why our numerical evaluation of Eq. (27) for σ_T depends only weakly on the infrared cutoff[10] K_0^2. Indeed, integral (26) for σ_L is controlled by contributions close to the upper limit and we expect

$$\frac{d^2\sigma_L}{dM^2dt}\sim\frac{(Q^2)^{2\gamma-2\lambda}}{Q^6}. \tag{34}$$

This is exactly the same Q^2 behavior as the prediction (17) for *exclusive* ρ_L electroproduction; here, we have been more precise and displayed the Q^2 dependence coming from the $x(\simeq Q^2/W^2)$ behavior of the gluon. Of course, the result (34) is very approximate and the detailed dependence of the Q^2 behavior of σ_L (as well as of σ_T) on the properties of the gluon must await the numerical predictions of Sec. VI.

Nevertheless, we can take the general discussion further and anticipate the main features of the Q^2 behavior of the important ratio σ_L/σ_T. We first rewrite Eqs. (26) and (27) in terms of an integration over the angles of the produced $q\bar{q}$ pair. We use the polar angle θ of the outgoing q in $q\bar{q}$ rest frame with respect to the incident direction of the proton. Thus, we have

$$k_T=\tfrac{1}{2}M\sin\theta, \tag{35}$$

and the square root in the denominators of Eqs. (26) and (27) is equal to $\cos\theta$. Also the factor in the numerator of Eq. (27)

[9]In the qualitative discussion we omit, for simplicity, factors $2\beta-1$ and β in $I_L^{\rm LLA}$ and $I_T^{\rm LLA}$, respectively, which is appropriate for $Q^2 \gg M^2$.

[10]In Sec. VI we choose $K_0=0.2$ GeV, the order of the inverse confinement radius 1 fm^{-1}.

$$1-2\beta K^2/Q^2=\tfrac{1}{2}(1+\cos^2\theta)=|d^1_{11}(\theta)|^2+|d^1_{1-1}(\theta)|^2, \tag{36}$$

where $d^J_{\lambda\mu}(\theta)$ are the conventional spin rotation matrices. Then, Eqs. (26) and (27) become

$$\frac{d^2\sigma_L}{dM^2dt}=\frac{4\pi^2e_q^2\alpha}{3}\frac{Q^2}{(Q^2+M^2)^2}\frac{1}{8}\int_{-1}^{1}d\cos\theta|d^1_{10}(\theta)|^2|I_L|^2, \tag{37}$$

$$\frac{d^2\sigma_T}{dM^2dt}=\frac{4\pi^2e_q^2\alpha}{3}\frac{M^2}{(Q^2+M^2)^2}\frac{1}{4}\times\int_{-1}^{1}d\cos\theta[|d^1_{11}(\theta)|^2+|d^1_{1-1}(\theta)|^2]|I_T|^2, \tag{38}$$

where the dependence on the rotation matrices appropriately reflects the decay of the ρ meson from longitudinally and transversely polarized states, respectively.

In the limit of no interaction with the proton (that is, $I_L=I_T=\text{const}$, where the first equality assumes $Q^2\gg M^2$), the photon has to produce the $q\bar{q}$ pair in a pure spin $J=1$ state. We immediately find from Eqs. (37) and (38) that

$$\frac{\sigma_L}{\sigma_T}=\frac{Q^2}{2M^2}\frac{\int d\cos\theta\sin^2\theta}{\int d\cos\theta(1+\cos^2\theta)}=\frac{Q^2}{4M^2}. \tag{39}$$

In the realistic situation, the two-gluon exchange interaction distorts the $q\bar{q}$ state produced by the ''heavy'' photon. Some idea of the consequences of this distortion can be anticipated from the leading log approximation (31) for I_L and I_T, in which

$$I_L=I_T\sim\frac{(K^2)^\gamma}{K^2}\sim\frac{1}{(\sin^2\theta)^{1-\gamma}}. \tag{40}$$

We substitute this behavior into Eqs. (37) and (38), and project[11] out the spin-1 components of the underlying $q\bar{q}$ production amplitudes $[\sim d^1_{1\lambda}(\theta)I(\theta)$ where $I_L=I_T\equiv I(\theta)$ $\sim(\sin^2\theta)^{\gamma-1}]$. We then use the identity

$$\int_0^\pi\sin^p\theta\,d\theta=\sqrt{\pi}\frac{\Gamma\left(\frac{1}{2}+\frac{1}{2}p\right)}{\Gamma\left(1+\frac{1}{2}p\right)} \tag{41}$$

to evaluate the projections

$$c(\lambda)=\frac{2J+1}{2}\int d\cos\theta[d^{J=1}_{1\lambda}(\theta)I(\theta)]d^{J=1}_{1\lambda}(\theta), \tag{42}$$

assuming that γ is a constant over the region of integration. With this assumption we find the interesting result

$$\frac{\sigma_L}{\sigma_T}=\frac{Q^2}{2M^2}\frac{|c(\lambda=0)|^2}{|c(\lambda=1)|^2+|c(\lambda=-1)|^2}=\frac{Q^2}{M^2}\left(\frac{\gamma}{\gamma+1}\right)^2. \tag{43}$$

The dependence on γ has the effect of masking the Q^2 growth of σ_L/σ_T. This can be seen by inspecting Fig. 3; higher Q^2 means larger x and both changes imply smaller γ. The projection integrals (42) for the amplitudes [with their linear dependence on $I_i(\theta)$] are more infrared convergent than Eqs. (37) and (38). Now, σ_T (as well as σ_L) is convergent provided only that $\gamma>0$ as $K^2\to0$ (that is, as $\theta\to0$). In fact, provided x remains sufficiently small, both the σ_L and σ_T integrations receive their main contributions from the region $K^2\lesssim Q^2/4$, and so we should insert into Eq. (43) the average γ sampled in this x, K^2 domain. Indeed, the decrease of γ with increasing $K^2\lesssim Q^2/4$ is found to considerably suppress the growth of σ_L/σ_T with increasing Q^2, and to largely remove the gross disagreement of the QCD prediction with the data; see the full numerical calculation presented in Sec. VI. We may turn the argument the other way round. Accurate measurements of the ratio σ_L/σ_T as a function of Q^2 will offer an excellent way of constraining the K^2 and x behavior of the gluon $g(x,K^2)$ in the region $K^2\lesssim Q^2/4$ and $x\approx Q^2/W^2$. Of course, result (43), which is based on a constant γ, is oversimplified. It is given only to indicate the general trend. The full calculation of Sec. VI is performed with a realistic gluon distribution and so automatically allows for the K^2 (and x) dependence of γ.

We see that the projection integrals (42) converge in the infrared region of small $K^2\approx\frac{1}{4}Q^2\sin^2\theta$ [that is, at small θ] for any $\gamma>0$, even for σ_T [that is, for $c(\lambda=\pm1)$]. We have stronger infrared convergence for σ_L or $c(\lambda=0)$ due to $d^1_{10}=-\sin\theta/\sqrt{2}$. We also notice that the factor $I(\theta)=1/(\sin^2\theta)^{1-\gamma}$, arising from the $q\bar{q}$-proton interaction, gives a strong peak in the forward direction.[12] It means that the distortion caused by the interaction will, in principle, produce higher spin $q\bar{q}$ states. Most probably, the higher spin states at small M^2 are killed by confinement during the hadronization stage as there is insufficient phase space to create 2π states with large spin with $M^2\lesssim1$ GeV^2. In any case, the higher spin components[13] cannot affect ρ production, since confinement cannot change the spin of the produced $q\bar{q}$ state. At higher energies (small x), the anomalous dimension γ grows and the function $I(\theta)$ is not so singular as $\theta\to0$. Therefore, in this energy domain the incoming spin of the $q\bar{q}$ system is not so contaminated by $J\neq1$ components arising from the interaction with the proton. In the black disk

[11]To be precise, the rotation matrices $D^J_{\lambda\mu}(\phi,\theta,-\phi)$ form the orthogonal basis and we project out the components $c(\lambda)$ from the $q\bar{q}$ amplitudes $D^{1*}_{1\lambda}I(\theta)$ with the matrix $D^1_{1\lambda}$. However, the ϕ integrations are trivial and hence the projection can be done simply in terms of $d^1_{1\lambda}$.

[12]The height of the peak is limited by the infrared cutoff, $K_0=0.2$ GeV, provided by confinement.

[13]Indeed, it will be interesting to study the detailed spin decomposition of $\gamma^*\to$ open $q\bar{q}$ production as a function of M^2. In this way we can investigate how the QCD ''Pomeron'' distorts the initial state and how confinement or parton-hadron duality operates in different (relatively small) M^2 regions for the different J^P states.

limit of the proton, when the cross section approaches the saturation (unitarity) limit, γ tends to 1 and we come back to pure $J=1$ $q\bar{q}$ production.

VI. NUMERICAL QCD PREDICTIONS FOR ρ ELECTROPRODUCTION

We use parton-hadron duality to predict ρ electroproduction from the QCD formulas for open $u\bar{u}$ and $d\bar{d}$ production. To be precise we compute

$$\sigma_{L,T}(\rho)=0.9\int_{(0.6\ \mathrm{GeV})^2}^{(1.05\ \mathrm{GeV})^2} dM^2 \frac{d\sigma_{L,T}(J=1)}{dM^2}, \qquad (44)$$

where $d\sigma_{L,T}(J=1)/dM^2$ are the spin-1 projections of open $q\bar{q}$ production of Eqs. (37) and (38), carried out as described in Eq. (42), and where the cross sections have been integrated over t assuming the form $\exp(-b|t|)$ with the observed slope $b=5.5\ \mathrm{GeV}^{-2}$ [1,2]. The factor 0.9 is included in Eq. (44) to allow for ω production. The I_L and I_T integrations over the gluon transverse momentum are computed from Eqs. (28) and (29) as described in Ref. [16]. We checked the stability of the results to contributions from the infrared regions of the dK^2 and $d\ell_T^2$ integrations. First, we varied the infrared cutoff around the value $K_0=200$ MeV that we used to evaluate Eqs. (26) and (27). Second, we explored the effect of varying ℓ_0^2 around the value $\ell_0^2=1.5\ \mathrm{GeV}^2$ that we used to evaluate the integrals of Eqs. (28) and (29). Recall that we use the linear approximation described in Ref. [16] to evaluate the contribution from the region $\ell_T^2<\ell_0^2$. We found only a weak sensitivity to variation of the choice of ℓ_0^2. For instance, reducing ℓ_0^2 to 1 GeV^2 changes the cross sections by less than 5%. We will report on the sensitivity to variation of K_0 at the end of the section.

We begin by taking the gluon distribution from the MRS(R2) set of partons [7], which corresponds to a QCD coupling which satisfies $\alpha_S(M_Z^2)=0.12$. The parton set with this QCD coupling, found by global analysis of deep inelastic and related data (including recent HERA measurements of F_2), is favored by the Fermilab jet data with $E_T<200$ GeV [7]. We first compare our cross section predictions obtained with this gluon with the data. Then, we use different gluon distributions from several recent sets of partons to study the sensitivity of $\gamma^*p\to\rho p$ to the behavior of the gluon.

Note that we use phenomenological gluon distributions which are obtained from global fits to deep inelastic experimental data, rather than ''*ab initio*'' distributions calculated from theoretical models. Thus, the gluon distributions that we use already incorporate absorptive effects.

There is another crucial ingredient in the calculation of the cross section for diffractive open $q\bar{q}$ production. Virtual gluon corrections to the process shown in Fig. 2 are surprisingly important. The relevant diagrams are discussed in Ref. [16] and lead to π^2 enhancements of the $O(\alpha_S)$ corrections. If the contributions are resummed they lead to an enhancement of the lowest order result by a factor $\exp(\alpha_S C_F \pi)$, the so-called K factor enhancement, where the color factor $C_F=4/3$. A similar K factor is well known in Drell-Yan

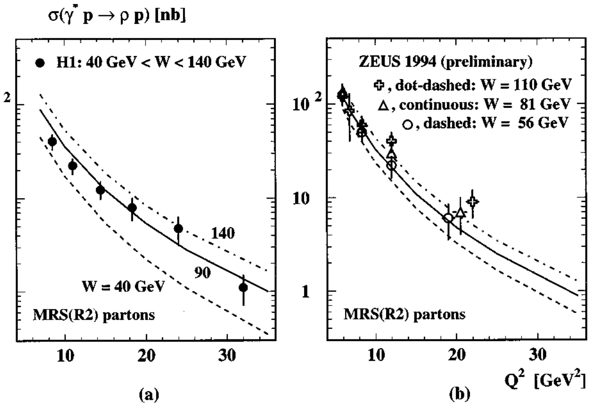

FIG. 4. The predicted Q^2 dependence of the cross section for $\gamma^*p\to\rho p$ compared with (a) H1 data [1] collected over the energy range $40<W<140$ GeV and (b) preliminary ZEUS data [3] in energy bins with $\langle W\rangle=56$, 81, and 110 GeV. The QCD curves for the various values of W are obtained using MRS(R2) partons [7].

production, although there the contributions come from different virtual diagrams [16]. For the Drell-Yan process the enhancement can be as much as about a factor of 3. In our case the K factor can, at present, only be estimated. It proves to be the main uncertainty in the normalization of diffractive $q\bar{q}$ production. The major ambiguity is associated with the choice of the argument of α_S. We take the scale to be $2K^2$. Since the K^2 integrations are dominated by contributions towards the upper limit, this choice is equivalent to a scale $\lesssim Q^2/2$. With this choice we obtain the values of the $\gamma^*p\to\rho p$ cross section shown by the curves in Fig. 4, which are in reasonable agreement with the measured values. For our choice of scale the average K factor for σ_L varies from about 3–3.7 for Q^2 going from 25–10 GeV^2, and is about 20–25% larger for σ_T (as in this case somewhat lower K^2 values are sampled). The cross section agreement shown in Fig. 4 corresponds to a physically reasonable choice of scale, and leads to a sensible range of size of the K factors. It shows that the open $q\bar{q}$ duality model for ρ electroproduction is at least consistent with observations. Due to the sensitivity to the choice of scale, clearly the agreement cannot be regarded as confirmation of the approach. Nevertheless, it does imply the existence of a sizable π^2 enhancement of the Born amplitude, as was also found in the Drell-Yan process.

On the other hand, the predictions for the Q^2 dependence of the ratio σ_L/σ_T have much less ambiguity. The calculations are compared with the measurements at HERA in Fig. 5. The agreement with the data shows a dramatic improvement over the QCD expectations which involve convolution with the ρ meson wave function. The small x behavior of the gluon plays a crucial role in masking the Q^2 increase anticipated in these earlier predictions of the ratio.

The dependence on the gluon is seen in Fig. 6 which compares the Q^2 behavior for σ_L/σ_T at $W=90$ GeV for the gluon distribution of several recent sets of partons [MRS(A′) [6], Glück-Reya-Vogt (GRV) [18], MRS(R2) [7]]. We stress that the normalization of the QCD predictions for the cross section are dependent on the choice of the mass interval embracing the ρ meson and on the estimate of the

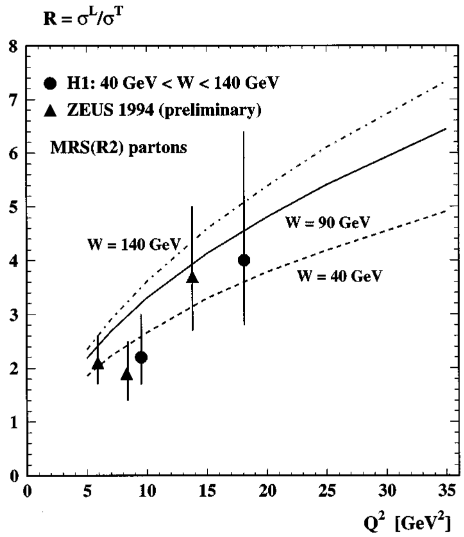

FIG. 5. The Q^2 dependence of the QCD predictions for the ratio σ_L/σ_T of the electroproduction of ρ mesons ($\gamma^* p \rightarrow \rho p$) in longitudinal and transverse polarization states compared with the most recent H1 [1] and ZEUS [3] data. MRS(R2) partons [7] are used.

K factor enhancement. On the other hand, the ratio σ_L/σ_T is not so sensitive to these ambiguities. At this stage it is relevant to study the stability of the results to variation of the infrared cutoff K_0. This we also show in Fig. 6, where we present QCD predictions based on MRS(R2) partons for two different choices of K_0. We see that the cross section is hardly changed while the ratio σ_L/σ_T increases a little when K_0 is increased from 200 to 300 MeV. Such a result is to be anticipated as σ_T samples, on average, smaller K^2 values than those by σ_L. However, we see that the sensitivity of the predictions for σ_L/σ_T to the value of K_0 is sufficiently weak so that measurements of the ratio can give a reliable probe of the gluon.

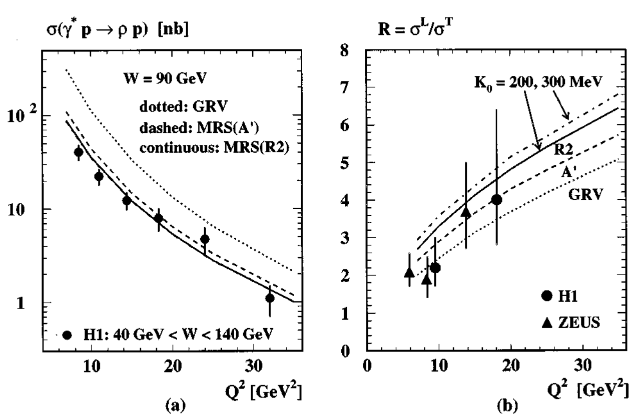

FIG. 6. The QCD predictions for $W=90$ GeV based on three recent sets of partons [6,7,18] compared with the recent HERA data [1,3]. We also show the sensitivity of the predictions using the MRS(R2) partons to the choice of the cutoff K_0; the dot-dashed curves correspond to $K_0=300$ MeV whereas all other curves correspond to $K_0=200$ MeV. The dot-dashed curve in (a) essentially coincides with the continuous curve which demonstrates the insensitivity of the cross section prediction to the value of K_0, whereas we see that the ratio σ_L/σ_T of (b) has some dependence.

VII. CONCLUSIONS

We have shown that the diffractive electroproduction of ρ mesons at high Q^2 can be described by perturbative QCD. Indeed, since ρ production in both longitudinally and transversely polarized states is being measured at HERA with better and better precision, the process $\gamma^* p \rightarrow \rho p$ can serve as an excellent testing ground for QCD. Moreover, we have shown that it also provides a sensitive probe of the small x behavior of the gluon distribution.

The validity of perturbative QCD is ensured by the large value of Q^2. This is already suggested by several features of the existing data [1,2,4]. However, the measurements of the ratio σ_L/σ_T do not support the behavior,

$$\frac{\sigma_L}{\sigma_T} \sim \frac{Q^2}{2m_\rho^2}, \tag{45}$$

predicted from QCD by convoluting $\gamma^* \rightarrow q\bar{q}$ diffractive production with our knowledge of the ρ meson wave function. The main problem is that the predictions for σ_T are too small and fall off too quickly with increasing Q^2. We showed that a nonperturbative approach to σ_T does not resolve the conflict with the data. Rather, we argued that on account of the low mass of the ρ meson the convolution with the wave function should be omitted. The $u\bar{u}$ or $d\bar{d}$ pairs produced in the ρ mass region have, because of phase space restrictions, little alternative but to hadronize as 2π states. Thus, a more appropriate approach to ρ electroproduction is to apply the parton-hadron duality hypothesis to open $u\bar{u}$ and $d\bar{d}$ production. Indeed, we found that this model gives a good description of all of the features observed for diffractive ρ electroproduction at HERA including, in particular, the Q^2 behavior of σ_L/σ_T. To gain insight into expectations of the model, we first made a simple estimate based on assuming a constant anomalous dimension γ. We found

$$\frac{\sigma_L}{\sigma_T} = \frac{Q^2}{M^2}\left(\frac{\gamma}{\gamma+1}\right)^2, \tag{46}$$

where M is the invariant mass of the $q\bar{q}$ pair and γ is the effective anomalous dimension of the gluon defined by $xg(x,K^2) \sim (K^2)^\gamma$, where the typical K^2 sampled is $K^2 \lesssim Q^2/4$ (approximated to be the same for both σ_L and σ_T). The decrease of γ with increasing Q^2 masks the strong growth shown in Eq. (45). Of course, result (46) is greatly oversimplified but it gives a good idea of the crucial role played by the gluon distribution. In Figs. 4–6 we showed the results of the full calculation. The computation is based on a measured gluon distribution and so automatically allows for the appropriate K^2 and x dependence of γ. The figures compare the detailed predictions of the model with the measurements of diffractive ρ electroproduction at HERA. The main uncertainty is in the normalization of the cross section. One source is in the choice of the width of the ΔM^2 interval over which to apply the duality hypothesis. The second is associated with the K factor enhancement which arises from virtual gluon corrections to open $q\bar{q}$ production. The normalization is sensitive to the choice of scale used as the argument of α_S in the calculation of the K factor. The data show evidence for a K factor of about 3–4, comparable in size to the K factor enhancement established for Drell-Yan production.

The QCD model prediction of the ratio σ_L/σ_T is essentially free of the above ambiguities. Figure 6 shows that precise measurements of the ratio for ρ electroproduction at different values of Q^2, and the $\gamma^* p$ c.m. energy W, will provide a valuable probe of the behavior of the gluon distribution $g(x,K^2)$ in the kinematic domain $x \approx Q^2/W^2$ and $K^2 \lesssim Q^2/4$.

ACKNOWLEDGMENTS

We thank E. M. Levin and R. G. Roberts for useful discussions and H. Abramowicz, A. Caldwell, B. Clerbaux, and A. De Roeck for information about the HERA data. M.G.R. thanks the Royal Society for financial support and T.T. thanks the U.K. Particle Physics and Astronomy Research Council for support. This research was also supported in part (M.G.R.) by the Russian Fund of Fundamental Research No. 96 02 17994.

[1] H1 Collaboration, S. Aid *et al.*, Nucl. Phys. **B468**, 3 (1996).
[2] ZEUS Collaboration, M. Derrick *et al.*, Phys. Lett. B **356**, 601 (1995).
[3] ZEUS Collaboration, N. Brummer, in Proceedings of the XXVIIIth International Conference on High Energy Physics, Warsaw, Poland, 1996 (unpublished).
[4] NM Collaboration, M. Arneodo *et al.*, Nucl. Phys. **B429**, 503 (1994).
[5] H1 Collaboration, S. Aid *et al.*, Nucl. Phys. **B470**, 3 (1996); ZEUS Collaboration, M. Derrick *et al.*, Z. Phys. C **69**, 607 (1996); Report No. DESY-96-076, hep-ex/9607002 (unpublished).
[6] A. D. Martin, R. G. Roberts, and W. J. Stirling, Phys. Lett. B **354**, 155 (1995).
[7] A. D. Martin, R. G. Roberts, and W. J. Stirling, Phys. Lett. B **387**, 419 (1996).
[8] M. G. Ryskin, Z. Phys. C **57**, 89 (1993).
[9] S. J. Brodsky *et al.*, Phys. Rev. D **50**, 3134 (1994).
[10] M. Genovese, N. N. Nikolaev, and B. G. Zakharov, Phys. Lett. B **380**, 213 (1996).
[11] E. C. Poggio, H. R. Quinn, and S. Weinberg, Phys. Rev. D **13**, 1958 (1976); Yu. L. Azimov *et al.*, Z. Phys. C **27**, 65 (1985); **31**, 213 (1986); Yu. L. Dokshitzer, V. A. Khoze, and S. I. Troyan, *ibid.* **55**, 107 (1992).
[12] D. Yu. Ivanov, Phys. Rev. D **53**, 3564 (1996); I. F. Ginzburg, D. Yu. Ivanov, and V. G. Serbo, Novosibirsk Report No. IM-TP-208, 1995, hep-ph/9508309 (unpublished); I. F. Ginzburg and D. Yu. Ivanov, Phys. Rev. D **54**, 5523 (1996).
[13] V. L. Chernyak and I. R. Zhitnitsky, Phys. Rep. **112**, 173 (1984).
[14] P. Ball and V. Braun, Phys. Rev. D **54**, 2182 (1996).
[15] V. N. Gribov, Sov. Phys. JETP **30**, 709 (1970); L. L. Frankfurt and M. I. Strikman, Phys. Lett. **65B,** 51, (1976).
[16] E. M. Levin, A. D. Martin, M. G. Ryskin, and T. Teubner, Z. Phys. C (to be published).
[17] N. N. Nikolaev and B. G. Zakharov, Z. Phys. C **49**, 607 (1991); Phys. Lett. B **260**, 414 (1991); Z. Phys. C **53**, 331 (1992); J. Bartels, H. Lotter, and M. Wüsthoff, Phys. Lett. B **379**, 239 (1996); E. Gotsman, E. M. Levin, and U. Maor, Report No. CBPF-NF-021/96, TAUP-2338-96, hep-ph/9606280 (unpublished).
[18] M. Glück, E. Reya, and A. Vogt, Z. Phys. C **67**, 433 (1995).